The Effect of End Sill on Submerged Spatial Hydraulic Jump: A Three-dimensional Numerical Study

Eng. Ahmed S. Foda, Dr. Yehya E. Imam, and Prof. Abdallah S. Bazaraa

Cairo University, Engineering, Irrigation and Hydraulics Department

الملخص العربى

تمت دراسة استقرار القفزة الهيدروليكية المغمورة المتكونة عند الاتساع الحاد في عرض قناة دخولاً لأحواض تهدئة ذات أو بدون عتب نهاية. تم إجراء محاكاة عددية ثلاثية الأبعاد بقيم مختلفة لارتفاع و مكان عتب النهاية. وجد أن ارتفاع و مكان عتب النهاية لهما دور هام في شكل و نمط القفزة الهيدروليكية، وتبديد الطاقة. أثبتت الدراسة أيضاً أن عتب النهاية لها دور فعال في استقرار القفزة الهيدروليكية المغمورة ذات النمط المتذبذب عند الاتساع الحاد في عرض قناة.

Abstract

Stability of submerged spatial hydraulic jumps below abrupt symmetric expansions are numerically studied for basins with and without end sills. Numerical simulations with different continuous sill heights and locations were conducted. Both parameters, sill height and sill location, were found to play an important role in the hydraulic jump configuration, energy dissipation, and flow patterns. End sill proved to be an efficient tool in stabilizing oscillatory submerged spatial hydraulic jump and reducing the jump length.

1. Introduction.

Many researchers studied intensively the free and submerged hydraulic jumps downstream of abrupt symmetric expansions (Herbrand, 1973; Ohtsu and Yasuda, 1991; Bremen and Hager, 1993; Zare and Baddour, 2007). There are many types of three dimensional hydraulic jumps that have been investigated downstream of abrupt symmetric expansions. The researchers classified the three dimensional hydraulic jump, by maintaining steady flow conditions upstream of the expansion and gradually increasing the tailwater depth, into repelled, spatial, transitional, and submerged spatial jumps (Figure 1) (Rajaratnam and Subramanya, 1968). A repelled jump develops downstream of the expansion section (Figure 1(a)) and is not recommended for its extreme basin length. A spatial jump occurs when the jump toe touches the expansion section (Figure 1(b)) and is not recommended for its unstable flow. A transitional jump develops when the jump advances upstream of the expansion section (Figure 1(c)). When tailwater depth is large, a submerged jump is formed. For piers of negligible length, a high tailwater depth leads to the formation of a submerged spatial hydraulic jump (SSHJ) (Figure 1(d)). Depending on flow symmetry and steadiness, several SSHJ types were observed in rectangular stilling basins (Ohtsu et al. 1999).
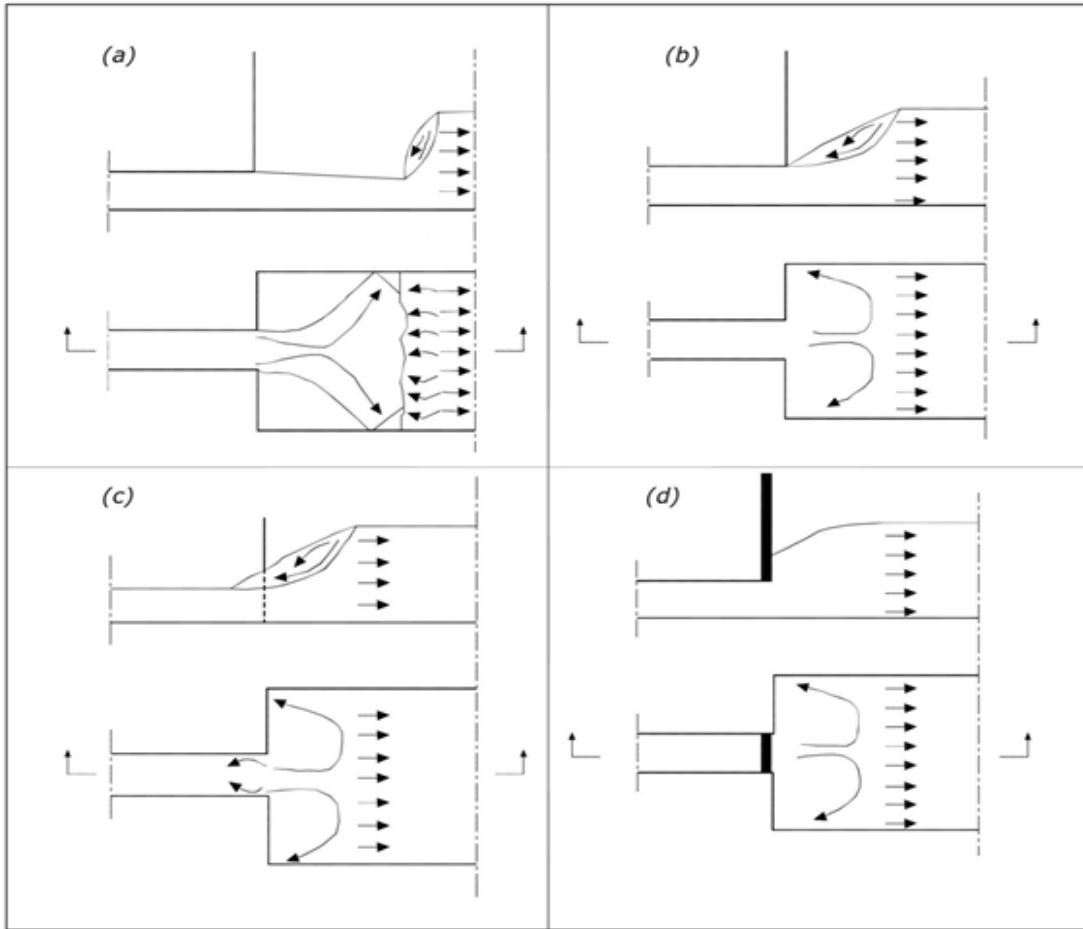
Figure (1) Section elevation and top view of jump classifications in an abrupt channel expansion: (a) repelled jump; (b) spatial jump (S-jump); (c) transitional jump; (d) submerged spatial jump.
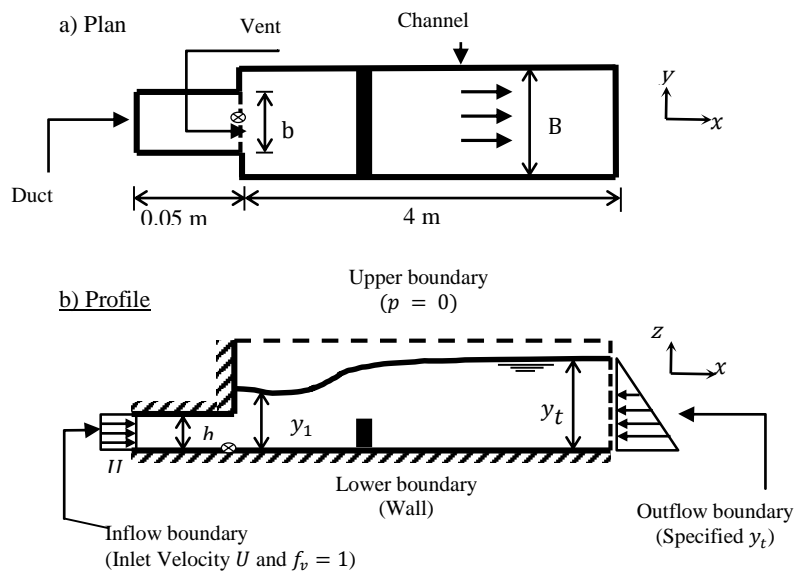

Figure (2) Schematic of a stilling basin with an end sill downstream of an abrupt expansion. Shown are the geometry and boundary conditions for the numerical domain in a) plan view and b) profile view through vent. Coordinate system x, y, and z has the origin indicated by the marker ⊗.

Appurtenances are typically inserted in stilling basins to force hydraulic jumps to develop closer to the inlet, therefore reducing the length of the basin (Figure 2). Common appurtenances are continuous and dentated sills across stilling basins. Hydraulic jumps affected by appurtenances have been intensively investigated and referred to as forced hydraulic jumps (Bradley and Peterka, 1957; Rajaratnam and Murahari, 1971; Rajaratnam and Hurtig, 2000; Achour and Debabèche, 2003; Debabeche et al., 2008). Continuous sills have been found in many studies to be the most effective appurtenance in reducing stilling basin length and increasing flow stability (Bremen and Hager, 1993). The effectiveness of a continuous sill depends on the sill height s and the sill location from the toe of the jump L_s. Zare and Doering (2010) studied experimentally the forced hydraulic jumps below abrupt symmetric and asymmetric expansions. Their experiments were limited to different two expansion ratios with different continuous sill heights and locations. Zare and Doering (2010) provided empirical equations to predict the sequent depth and the basin length at any sill height and sill location. Meshkati et al. (2012) experimentally studied the effect of end sill of length less than the channel width downstream the so-called in-ground stilling basin on the energy dissipation and sequent depth of hydraulic jump below abrupt symmetric expansion. These authors provided a design guideline considering downstream flow conditions.

As forced SSHJ is the critical case of the transitional jump and can happen for different operating conditions, the current study aims to numerically simulate forced SSHJ jump with continuous sills of different heights s and locations L_s. Effect of end sill on stabilizing the oscillatory asymmetric SSHJ was studied. A parameter proposed by Zare and Doering (2010), relating the sill height together with the sill location, is used and employed to give conditions at which end sill is effective in stabilizing the oscillatory SSHJ. This paper is structured as follows. The following section describes the numerical model and its application. Next, numerical model results are presented. Finally, we discuss the numerical model results, the effect of end sill on the oscillatory hydraulic jump stability, the role of the end sill in reducing the jump length and increasing energy dissipation.

2. Methods

2.1 Numerical Model Setup and Application
Computational fluid dynamics (CFD) are widely used nowadays in simulating hydraulics engineering problems. Different cases of simulations were prepared to be numerically simulated to test the effect of end sill on the stabilization of submerged spatial hydraulic jump. ANSYS-FLUENT 14.5 software was used for the numerical simulation of three-dimensional turbulent flow downstream of single symmetric vent with the existence of end sill downstream of the expansion section. The flow is governed by incompressible continuity equation and Reynolds-averaged Navier– Stokes equations. Two-equation $k - \varepsilon$ turbulence closure model was used to compute the turbulent stresses (Akoz et al. (2009).

Numerical simulations were performed to test the effect of continuous end sill on oscillatory SSHJ (Table 1). Simulations were performed for one value of the expansion ratio, α = 0.33, and aspect ratio was β ≅ 5. Inlet Froude number, $F_r = U/\sqrt{gh}$, ranged between 3.02 and 5.43 where U is the average flow velocity through the vent, h is vent height, and g = 9.81 m/s² is gravitational acceleration. The sill height ratios HS = s/h

and the sill location ratios LS $= L_s/h$ were chosen to be from 1.0 to 4.0 and from 12.0 to 22.0, respectively (Zare and Doering, 2010). A parameter, relating the sill height together with the sill location (δ = HS/LS) (Zare and Doering, 2010), is employed to define the end sill ability in stabilizing the oscillatory SSHJ. The sill height to location ratio ranged between 0.045 for runs I-ES2 and I-ES6 and 0.333 for runs I-ES3 and I-ES7. A numerical simulation I-OA was carried out without the end sill to assess the effectiveness of the end sill. Simulations were performed in horizontal rectangular flume of 4.0 m length and 0.4 m width (Figure 2).

Table 1: Geometric and hydraulic parameters of numerical simulations

Run Code	B (m)	$\alpha = \dfrac{b}{B}$	$\beta = \dfrac{b}{h}$	F_r	y_t (m)	Sill Height Ratio ($HS = s/h$)	Sill Location Ratio ($LS = l_s/h$)	Sill Height to Location Ratio ($\delta = HS/LS$)
I-OA	0.4	1/3	5.03	3.02	0.115	0	0	-
I- ES1						1	12	0.083
I- ES2				3.02	0.115	1	22	0.045
I- ES3						4	12	0.333
I- ES4	0.4	1/3	5.03			4	22	0.182
I- ES5						1	12	0.083
I- ES6				5.43	0.149	1	22	0.045
I- ES7						4	12	0.333
I- ES8						4	22	0.182

To simulate the location and shape of the water free surface the VOF method was used. It uses a filling process to determine which cell in the grid is filled and which cell is emptied (Hirt and Nichols, 1981). A volume fraction field (F) is then defined in this grid, which can take values between 0 and 1, i.e., $F = 0$ if the cell is emptied and $F = 1$ when it is completely filled with liquid. A value of F between 0 and 1 means a fractional fill, with the free surface located within the cell. The VOF method can simulate the water free surface efficiently when the free surface is strongly enfolded (e.g. flow over spillways, weirs, sluices) (Nguyen and Nestmann, 2004).

At the inlet boundary, longitudinal velocity was applied uniformly over the vent cross section taking the vertical velocity component as zero. At the outlet boundary, free surface level was kept constant by assigning a specified tailwater depth at the downstream end of the channel. For channel bed and sides, the boundary condition was set as a wall (i.e., the perpendicular velocity is zero) (Figure 2).

2.2 Analysis of Model Results

An index was developed to measure the degree of symmetry (DSI) of submerged jump depending on the distribution of longitudinal velocity component across the channel cross section (Foda et al., submitted). Equation (1) describes the degree of symmetry index, DSI was calculated through the jump roller zone. The degree of symmetry index was calculated using,

$$DSI = \left(1 - \frac{\sqrt{\frac{1}{n}\Sigma(u_{left} - u_{right})^2}}{U}\right) \times 100\% \tag{1}$$

where u_{left} and u_{right} represent the longitudinal velocity component left and right of the longitudinal channel axis, respectively, and U is the magnitude of inlet velocity.

One of the most important engineering applications of the hydraulic jump is to dissipate energy in channels, regulators, and similar structures so that the excess kinetic energy does not damage these structures. The rate of energy dissipation or head loss across a hydraulic jump is a function of the hydraulic jump inflow Froude number and the height of the jump. The energy dissipation can be calculated using equation (2).

$$\frac{H_l}{H_o} = \frac{\left(y_1 + \frac{U^2}{2g}\right) - \left(y_t + \frac{U_t^2}{2g}\right)}{\left(y_1 + \frac{U^2}{2g}\right)} \tag{2}$$

where U and U_t represent the mean velocities upstream and downstream the jump respectively, y_1 is the water depth at toe of jump, y_t is the tail-water depth, and $g = 9.81$ m/s2 is gravitational acceleration.

The jump roller length is an important characteristic of the hydraulic jump as it determines the basin length of the hydraulic structure. The jump length is calculated in this study by contouring the roller extent using the values of longitudinal velocity component, where inside the roller the longitudinal velocity are negative and outside are positive. End sill is inserted in the stilling basin to reduce its length.

The effectiveness of the end sill is assessed by examining four aspects; whether the oscillatory SSHJ became steady or not, whether the SSHJ is symmetric or asymmetric, the reduction in roller length, and finally the increase in energy dissipation. The numerical model was validated using previous experimental results in the author's PhD thesis.

3. Results and Discussion

3.1 Flow symmetry

Model results for run I-ES1 with sill height ratio of HS = 1 and sill location ratio of LS = 12 indicated the formation of a steady symmetric jump (Figure 3). For the same vent geometry and flow conditions, and by increasing the sill location ratio from LS = 12 to 22 (shifting the sill away downstream the vent with the same height), run I-ES2 also generated a steady symmetric jump (Figure 3). In runs I-ES1 and I-ES2, along-channel velocity downstream of the expansion section was similar on both sides of the channel and the flow was steady without large-scale fluctuations (Figure 3). Simulations indicated the formation of an eddy roller just downstream the end sill.

By increasing the sill height ratio from HS = 1 to 4, the produced submerged spatial jump was steady asymmetric jump for the sill location ratio of LS = 12 in run I-ES3 and a steady symmetric jump for the larger sill location ratio of LS = 22 in run I-ES4 (Figure 4). In run I-ES3, along-channel velocity was steady with dissimilar distribution between the left and right sides of the channel (Figure 4a). In run I-ES4, the distribution of the longitudinal

velocity was symmetric about the channel centerline and the flow jet downstream the expansion section is steady. Side rollers were similar in size (Figure 4c).

From the preceding results, the end sill was found to be an efficient tool to stabilize the oscillatory SSHJ, and increase flow symmetry. In run I-ES3 with sill height to location ratio $\delta = 0.333$, the produced jump was not fully symmetric and stable, so it is not recommended to use end sill with sill height to location ratio more than 0.25. For smaller sill location ratio such as runs I-ES1 and I-ES3, the water surface rises above the end sill more than that of runs I-ES2 and I-ES4 with larger sill location ratio. For larger sill height ratio such as runs I-ES3 and I-ES4, the extent of the roller just downstream the end sill increases. Another group of runs have been carried out with different Froude number F_r and tail-water depth y_t to test the efficiency of end sill with different hydraulic parameters and the same performance of the previous group was found (i.e., by changing the inlet Froude number and tailwater depth simultaneously, the end sill with the same dimensions can stabilize the hydraulic jump and generate the same performance).
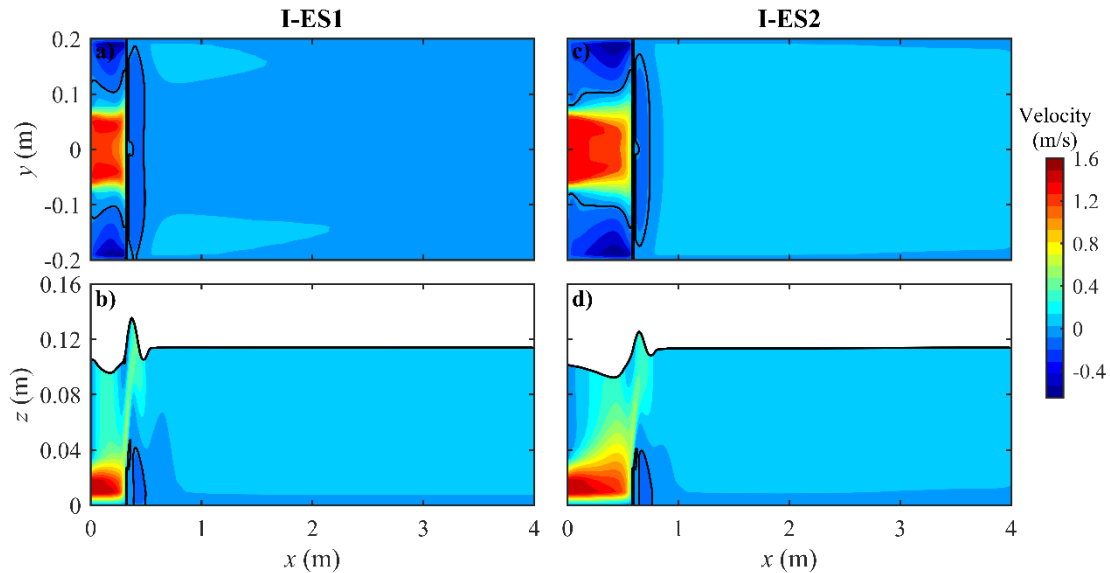

Figure (3) Distribution of longitudinal velocity over horizontal plane at height $z = 0.02$ m above bed and a longitudinal profile at $y = 0$ for run I-ES1, and run I-ES2.
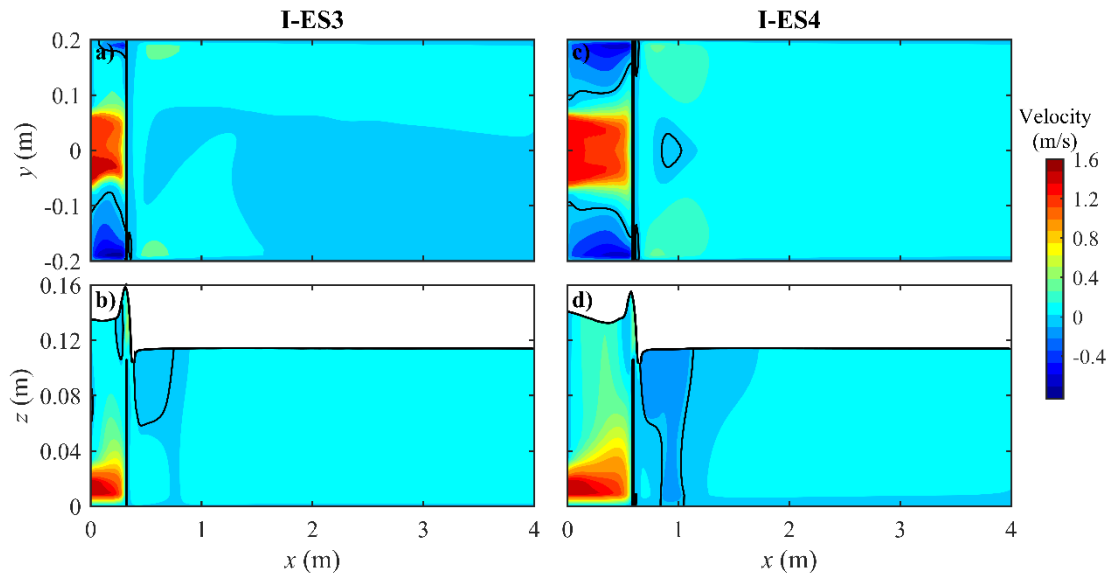
Figure (4) Distribution of longitudinal velocity over horizontal plane at height z = 0.02 m above bed and a longitudinal profile at y = 0 for run I-ES3, and run I-ES4.

Degree of symmetry index (DSI) based on longitudinal velocity distribution was calculated for all simulations and ranged between 61% and 98% (Figure 5). The lowest (DSI) values were around 61% and 67% and were for runs I-ES3 and I-ES7 respectively which simulated with end sill height to location ratio $\delta = 0.333$ (i.e., by increasing the sill height to location ratio the degree of symmetry index decreases). For runs I-ES1, I-ES2, I-ES4, I-ES5, I-ES6, and I-ES8, values of (DSI) were much higher ranging between 93% and 98%.
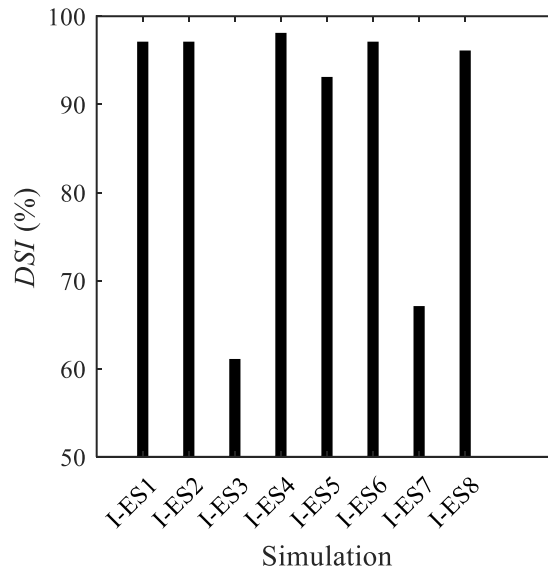
Figure (5) Degree of symmetry index for runs I-ES1, I-ES2, I-ES3, I-ES4, I-ES5, I-ES6, I-ES7, and I-ES8.

18

3.2 Jump length

The jump roller length was calculated using numerical simulations flow results. Simulation of run I-OA with no end sill indicated the jump roller length was equal to 1.76m. For sill location ratio LS = 12, model results for run I-ES1 with sill height ratio HS = 1 indicated that jump roller length is 1.16m and for run I-ES3 with sill height ratio HS = 4 the jump roller length is 1.21m. By increasing the sill location ratio from LS = 12 to 22, model results for run I-ES2 with sill height ratio HS = 1 indicated that jump roller length is 1.18m and for run I-ES4 with sill height ratio HS = 4 the jump roller length is 1.24m. Previous results indicated that by increasing the sill height ratio for the same sill location ratio the jump roller length increase. End sill is an effective tool in decreasing jump roller length by 30% for run I-ES4 to 34% for I-ES1.

3.2 Energy dissipation

Using equation (2) and the numerical simulation results the energy dissipation ratio was computed (Figure 6). For sill height ratio HS = 0, model results indicated that energy dissipation ratio for run I-OA is 0.24. For sill height ratio HS = 1, model results indicated that energy dissipation ratio for runs I-ES1 and I-ES2 is 0.34. By increasing the sill height ratio from HS = 1 to 4, energy dissipation ratio for runs I-ES3 and I-ES4 is 0.42. These results indicated that the energy dissipation ratio increases by increasing the sill height ratio. The sill location ratio has no effect on the energy dissipation. The energy dissipation rate when end sill exists is more than in the case with no end sill.
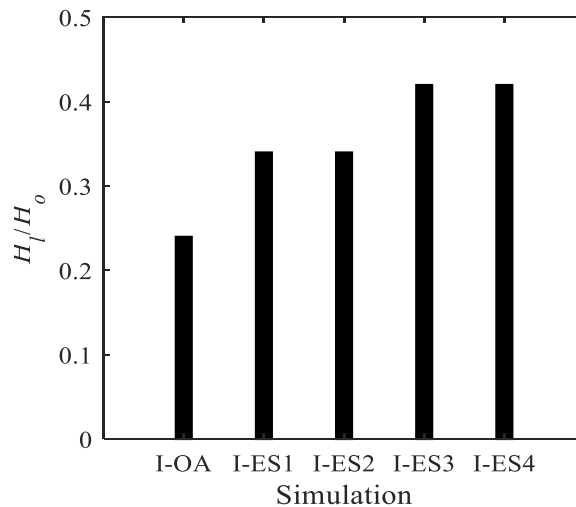

Figure (6) Energy dissipation ratio for runs I-OA, I-ES1, I-ES3, I-ES3, and run I-ES4.

3. Conclusions

Forced hydraulic jumps for the submerged spatial case were numerically investigated. The end sill is shown to be an efficient appurtenance to stabilize the oscillatory SSHJ and reduce jump roller length. End sill with sill height to location ratio more than 0.25 is not recommended because the produced jump is asymmetric. By increasing the sill height ratio for the same sill location ratio the jump roller length increases. The sill location ratio has no effect on the energy dissipation; however the energy dissipation ratio increases by increasing the sill height ratio.

4. References

1. Achour, B. and M. Debabèche (2003). "Control of hydraulic jump by sill in triangular channel." Journal of Hydraulic Research 41(3): 319-325.
2. Akoz, M. S., M. S. Kirkgoz and A. A. Oner (2009). "Experimental and numerical modeling of a sluice gate flow." Journal of Hydraulic Research 47(2): 167-176.
3. Bradley, J. N. and A. J. Peterka (1957). "The hydraulic design of stilling basins: hydraulic jumps on a horizontal apron (basin i)." Journal of the Hydraulics Division 83(5): 1-24.
4. Bremen, R. and W. H. Hager (1993). "T-jump in abruptly expanding channel." Journal of Hydraulic research 31(1): 61-78.
5. Debabeche, M., M. Lakehal, N. Mansri and B. Achour (2008). "Theoretical study of the forced hydraulic jump by positive step in a triangular channel." International Journal of Fluid Mechanics Research 35(4).
6. Herbrand, K. (1973). "The spatial hydraulic jump." Journal of Hydraulic Research 11(3): 205-218.
7. Hirt, C. W. and B. D. Nichols (1981). "Volume of fluid (VOF) method for the dynamics of free boundaries." Journal of computational physics 39(1): 201-225.
8. Meshkati, M. S., T. Sumi and S. X. Kantoush (2012). "The effect of end-sill geometry on functionality of in-ground stilling basin."
9. Nguyen, V. T. and F. Nestmann (2004). "Applications of CFD in hydraulics and river engineering." International Journal of Computational Fluid Dynamics 18(2): 165-174.
10. Ohtsu, I. and Y. Yasuda (1991). "Transition from supercritical to subcritical flow at an abrupt drop." Journal of hydraulic research 29(3): 309-328.
11. Rajaratnam, N. and K. I. Hurtig (2000). "Screen-type energy dissipator for hydraulic structures." Journal of Hydraulic Engineering 126(4): 310-312.
12. Rajaratnam, N. and V. Murahari (1971). "A contribution to forced hydraulic jumps." Journal of Hydraulic Research 9(2): 217-240.
13. Rajaratnam, N. and K. Subramanya (1968). "Hydraulic jumps below abrupt symmetrical expansions." Journal of the Hydraulics Division 94(2): 481-504.
14. Zare, H. K. and R. E. Baddour (2007). "Three-dimensional study of spatial submerged hydraulic jump." Canadian Journal of Civil Engineering 34(9): 1140-1148.
15. Zare, H. K. and J. C. Doering (2010). "Forced hydraulic jumps below abrupt expansions." Journal of Hydraulic Engineering 137(8): 825-835.